The Dimerization Stability of the HLH-LZ Transcription Protein Family Is Modulated by the Leucine Zippers: A CD and NMR Study of TFEB and c-Myc†

C. Muhle-Goll,*,‡ T. Gibson,‡ P. Schuck,§ D. Schubert,§ D. Nalis,‡ M. Nilges,‡ and A. Pastore‡

EMBL, Meyerhofstrasse 1, D-69117 Heidelberg, Germany, and Institut für Biophysik der Johann Wolfgang Goethe-Universität, D-60596 Frankfurt am Main, Germany

Received January 31, 1994; Revised Manuscript Received June 15, 1994®

ABSTRACT: In the HLH-LZ protein family, the helix–loop–helix DNA-binding dimerization domain is followed in the sequence by a leucine zipper motif. The precise function of this second dimerization domain is still unclear, since the HLH motif of a subset of this family has been shown to be necessary and sufficient for dimerization. However, deletion and mutagenesis studies of the leucine zipper in various HLH-LZ proteins have shown a clear influence of this motif on homo- and heterodimerization. In this paper, we present a structural characterization of synthetic peptides encompassing the leucine zipper sequences of c-Myc and TFEB, using circular dichroism, analytical ultracentrifugation, and nuclear magnetic resonance. We show that the different ability of the synthetic leucine zippers of c-Myc and TFEB to homodimerize at neutral pH reflects the different dimerization properties reported for the entire proteins. The TFEB protein is known to form homodimers. c-Myc, on the other hand, does not homodimerize in vivo, but is mostly found in heterodimeric complexes with Max, another protein of the HLH-LZ family. Accordingly, our results show that the TFEB peptide homodimerizes at neutral pH whereas the Myc peptide dimerizes to a comparable amount only at acidic pH and high ionic strength. Both synthetic peptides are far less stable than leucine zippers of the b-ZIP family. The relative stability of the two leucine zippers and the factors which stabilize the dimer formation are discussed.

Leucine zipper motifs are characterized by a repeat of leucines every seven residues within a sequence with a high tendency to fold as a helix. This motif was first recognized in a family of transcription activator proteins, named b-ZIP,[1] which dimerize through a leucine zipper domain and position a contiguous basic region to recognize and bind to a specific DNA sequence (Landschulz et al., 1988). Both the NMR and the X-ray structures of the leucine zipper domain from one member of this family (GCN4) have shown that it forms a parallel coiled coil (Oas et al., 1990; Saudek et al., 1990, 1991; Ellenberger et al., 1992). In the eukaryote yeast, leucine zipper domains appear to act primarily as homodimers while in complex multicellular organisms a large body of evidence indicates that the functional molecules most often form heterodimers (Hai et al., 1989; Mitchell & Tijan, 1989; Cao et al., 1991; Williams et al., 1991).

In the past years, there have been extensive investigations to determine the exact structural rules governing the choice of dimerization partners both for leucine zippers of members of the b-ZIP family [for a review, see Baxevanis and Vinson (1993)] and for model peptides derived from the tropomyosin coiled coil (Zhou et al., 1994, and references cited therein). There is a general agreement that specificity resides in the mostly hydrophobic *a* positions and the charged residues in *e* and *g* positions.

Since the first recognition of the leucine zipper domain, several unrelated families of proteins, some of which also function as transcription activators, have been suggested to contain leucine zipper dimerization domains. These occur in various contexts and in association with a range of different DNA-binding domains. In the HNF1 family, for instance, the leucine zipper domain is separated by a long intervening sequence from the DNA-binding domain (Frain et al., 1989; Nicosia et al., 1990). In the only known prokaryotic example, the LAC repressor of *Escherichia coli*, the leucine heptad repeats have the ability to form homomeric four helical bundles with an antiparallel arrangement of the helices (Alberti et al., 1993).

Yet another group of proteins, the HLH-LZ family, also possesses a leucine zipper (Dang et al., 1989; Beckmann et al., 1990; Carr & Sharp, 1990; Gregor et al., 1990; Hu et al., 1990). These proteins form a subgroup of what is known as the helix–loop–helix family (Murre et al., 1989). The HLH domain was originally defined on the basis of two strongly helical segments, interrupted by a nonconserved region of variable length. Dimerization—which is a prerequisite for DNA binding—is provided by the HLH motif. DNA specificity resides in the N-terminal basic region with conserved helical periodicity, indicating it to be an extension of helix-1 (Davis et al., 1990). The HLH-LZ family is characterized by an additional leucine zipper as a C-terminal extension of the DNA binding region which, according to an X-ray structure of one member of this group, Max, extends the second helix in a single continuous arrangement (Ferré-D'Amaré et al., 1993). Since the HLH motifs of proteins such as E12, E47, and MyoD have been shown to be necessary and sufficient for dimerization, the reason for the attached leucine zipper in the HLH-LZ subfamily has been rather unclear. However, it has been shown to have a strong effect on the choice of

† This work was supported by the Deutche Forschungsgemeinschaft (SFB169) (D.S. and P.S.).

* To whom correspondence should be addressed.

‡ EMBL.

§ Institut für Biophysik der Johann Wolfgang Goethe-Universität.

® Abstract published in *Advance ACS Abstracts,* September 1, 1994.

[1] Abbreviations: HLH, helix–loop–helix; LZ, leucine zipper; b-Zip, basic leucine zipper; Myc-LZ and TFEB-LZ, synthetic peptides spanning the sequence of the leucine zipper region of c-Myc and TFEB, respectively; CD, circular dichroism; NMR, nuclear magnetic resonance; TPPI, time–proportional phase incrementation; TOCSY, total correlation spectroscopy; NOE, nuclear Overhauser enhancement; NOESY, 2D NOE spectroscopy; TFE, trifluoroethanol; T_m, melting temperature.

0006-2960/94/0433-11296$04.50/0

dimerization partner in TFE3 (Beckmann & Kadesh, 1991), TFEB (Fisher et al., 1991), AP-4 (Hu et al., 1990), and USF (Gregor et al., 1990). In the latter case, Gregor et al. found a truncated form without an intact leucine zipper unable to homodimerize in the absence of DNA. Amati et al. (1993) generated Myc and Max mutants in the leucine zipper region by which they were able to change dimerization properties from hetero- to homodimerization. Thus, it seems that the leucine zippers have a distinct role from the HLH region notwithstanding the helical continuity observed in the 3D structure of Max.

In the present work, we have approached the role of the HLH-LZ leucine zippers through an investigation of their structural properties and relative stabilities. Two synthetic peptides spanning the leucine zipper sequences of two representative members of the HLH-LZ family, namely TFEB and c-Myc (hereafter referred to as Myc-LZ and TFEB-LZ), were synthesized and characterized by circular dichroism, analytical ultracentrifugation, and nuclear magnetic resonance studies.

MATERIALS AND METHODS

Amino Acid Sequences. Sequences were extracted from the SwissProt database (Bairoch & Boeckmann, 1991).

Peptide Synthesis. Solid-phase synthesis was performed on an Applied Biosystems 431A peptide synthesizer using Fmoc chemistry. DCC/HOBt activation and 4-(2′,4′-dimethoxyphenyl-Fmoc-aminomethyl)phenoxy resin with an initial substitution level of 0.39 mmol/g on a 0.1 mmol scale were used. Standard activation and protecting groups were used. After synthesis was completed, protecting groups were removed, and the peptide chains were cleaved from the resin eluting with TFA/phenol/EDT/thioanisole/water (10 mL: 0.75 g:0.25 mL:0.50 mL:0.50 mL) for 3 h.

The crude peptides were purified on a Vydac C-18 reverse-phase column (22 × 250 mm, 0.010 mm particles). Solvent A was water containing 0.1% TFA, and solvent B was 70% acetonitrile and 0.1% TFA in water. The linear gradient was from 30% to 40% of solvent B at a flow rate of 10 mL/min. Peptide purity (≥98%) was determined by HPLC using an acetonitrile gradient of 0.7%/min, and composition was confirmed by amino acid analysis and mass spectrometry.

Circular Dichroism Spectroscopy. Circular dichroism measurements were carried out on a Jobin Yvon Mark VI spectrometer fitted with a temperature-controlled Haake GH water bath and a Jasco J710 instrument equipped with a Neslab (Model RTE-100) water bath. Both spectrometers were calibrated using the ammonium salt of 10-(+)-camphor-sulfonic acid. Quartz cells of 0.2 and 1 mm path length were used. Spectra were obtained on samples containing between 2 and 2000 μM peptide at various pH values and salt concentrations. Unless otherwise specified, pH was adjusted by the addition of either suitable quantities of HCl (for acidic conditions) or of 20–50 mM Tris-HCl (for neutral conditions). Temperature scans were performed from 5 to 75 °C with 2 ± 0.2 °C steps. The ellipticity at 222 nm was recorded after the sample was allowed to equilibrate for at least 5 min after each temperature increase. Spectra shown are an average of 2–5 scans. The spectra were normalized for concentration and path length to obtain the mean residue ellipticity after subtraction of the buffer contribution. The spectra were processed with the program SNARF (van Hoesel, University of Groningen, 1992) and plotted with GNUPLOT.

Analytical Ultracentrifugation. Sedimentation equilibrium experiments were performed in a Beckman Optima XL-A analytical ultracentrifuge, using 12 mm Epon double sector centerpieces and sample volumes of 230 or 150 μL. The rotor speed was 40000 rpm, and the rotor temperature was 4 °C. Equilibrium was achieved after 73 and 35 h, respectively. The absorption profiles were recorded at 275 nm. The partial specific volume of 0.73 mL/g was calculated according to Reynolds and McCaslin (1985). TFEB-LZ was studied: (1) in 50 mM Tris-HCl, pH 7.2, and 10 mM NaCl, at peptide concentrations between 41 and 84 μM and (2) in 50 mM sodium acetate, pH 3.8, and 20 mM NaCl at concentrations between 47 and 71 μM. Least squares fits and the analysis of the statistical accuracy of the parameters (including the baseline position) were performed according to Schuck (1994) with the use of *F*-statistics (Johnson & Faunt, 1992).

Nuclear Magnetic Resonance Measurements. The NMR measurements were carried out using 2–4 mM samples both in 90% H_2O/10% D_2O and in 100% D_2O solutions. Different pH conditions (pH 3.0 and 5.9) were used to resolve overlapping resonances. 2D spectra were acquired at 7, 17, and 27 °C. The NMR spectra were recorded on 600 and 500 MHz Bruker AMX spectrometers.

2D spectra were recorded in phase-sensitive mode (Marion & Wüthrich, 1983) with water proton-frequency irradiation. Clean TOCSY spectra (Bax & Davis, 1985) were measured using the MLEV-16 composite pulse cycle (Rance, 1987) for the generation of the spin-lock field of (γB_2) = 10–11 kHz with 60 ms mixing time. Mixing times of 100 and 200 ms were used in the NOESY experiments (Jeener et al., 1979; Macura et al., 1981). Data were processed on a Bruker X32 station using the UXNMR program. The AURELIA program was used for displaying and plotting spectra. Slowly exchanging protons were identified by dissolving a fully protonated sample in D_2O and recording NOESY spectra after 2, 4, 6, and 8 h.

RESULTS

Choice of Leucine Zipper Peptides. Figure 1A shows an alignment of HLH-LZ sequences. In this study, we chose two leucine zipper sequences derived from proteins with different dimerization properties, namely, the zipper from TFEB, a protein which readily forms homodimers, and the one from c-Myc, which does not homodimerize except at very high concentrations (Fisher et al., 1991; Dang et al., 1989). Panels B and C of Figure 1 show schematic representation of the sequences in a helical wheel. Coiled coil positions are indicated.

Circular Dichroism Measurements. The far-ultraviolet CD spectra of both Myc-LZ and TFEB-LZ show characteristics of α-helical structure with two ellipticity minima around 208 and 222 nm (Figure 2). Two criteria were used in the analysis: the helical content and the degree of coiling. The first was calculated from the intensity of the molecular ellipticity at 222 nm in the normalized spectra, assuming that for a 100% helical peptide this value is $-33400°$ cm^2 dmol^{-1} (Chen et al., 1974). The degree of coiling was estimated from the ratio between the intensities of the bands at 222 and 208 nm. Changes of this ratio have been explained as follows: the n–π^* transition (222-nm CD band) is only responsive to the α-helical content. The π–π^* excitation band at 208 nm on the other hand polarizes parallel to the helix axis and is sensitive to whether the α-helix is monomeric or is involved in tertiary contacts as in the case of the dimeric coiled coil of leucine zippers (Cooper & Woody, 1990; Zhou et al., 1992a;

A

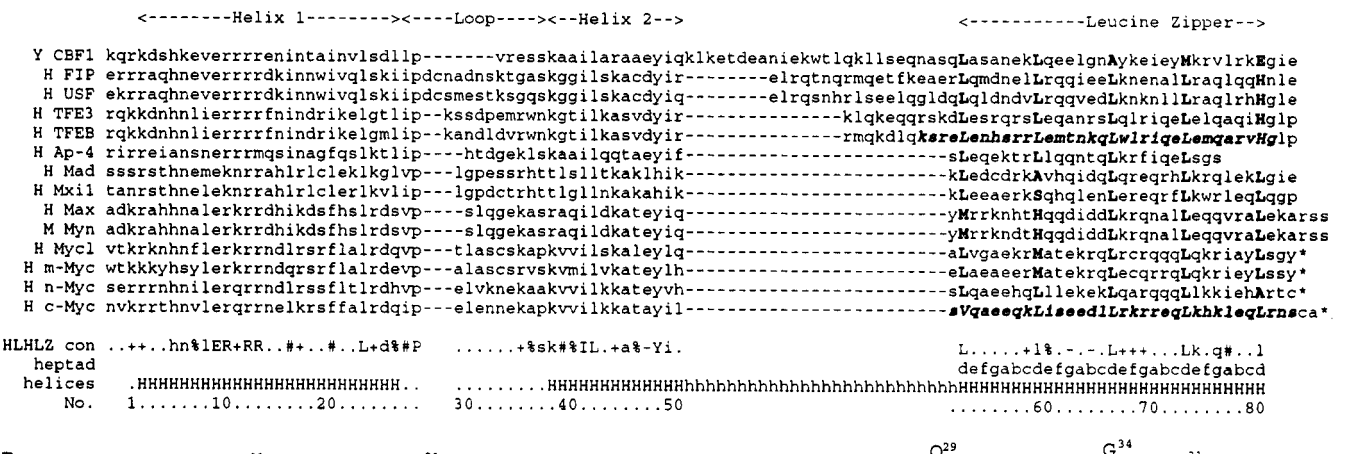

B

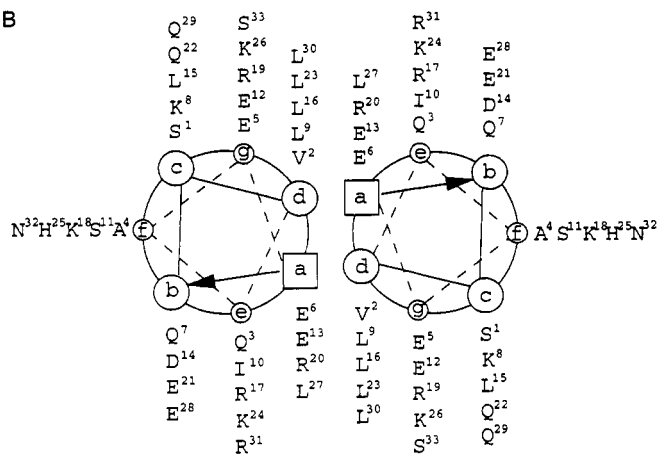

C

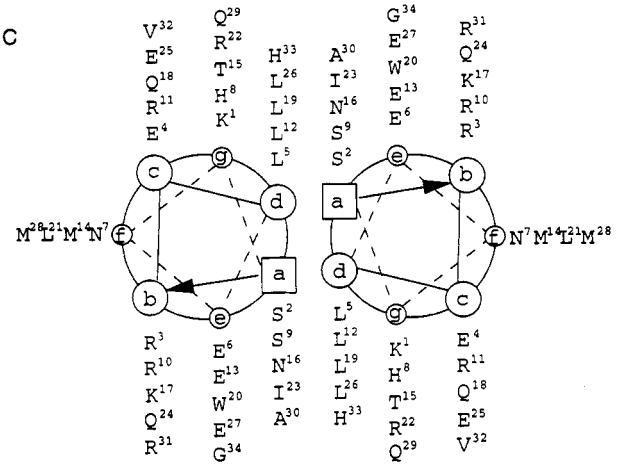

FIGURE 1: (A) Sequence alignment of HLH-LZ domains together with a derived consensus and helical assignments. The species names are annotated as follows: H, human; M, mouse; Y, yeast. Heptad periodic positions are indicated for the leucine zipper part in the usual helical wheel notation a–f. The *d* positions of the leucine zipper are marked with bold capital letters. The sequences of the synthetic leucine zipper peptides Myc-LZ and TFEB-LZ, used in this paper, are shown in bold italics. Symbols used for the consensus sequence, HLH-LZ con, are as follows: #, mostly hydrophobic residues; %, partially hydrophobic residues; +, usually positively charged residues; –, usually negatively charged residues. Capitals indicate strongly conserved residues. Helical residues are shown as H (definite) and h (probable). (B) Coiled coil helical wheel representation of the sequences of the Myc-LZ homodimer. Residues are numbered from 1 (N-terminus) to 33 (C-terminus). (C) The same for the TFEB-LZ homodimer [numbered from 1 (N-terminus) to 34 (C-terminus)].

Greenfield & Hitchcock-DeGregori, 1993). Monomeric α-helices show a higher intensity of the 208-nm band than interacting helices even though the α-helical content remains the same. Therefore, changes which enhance the ratio of the intensities of the two bands can be interpreted as an additional and more sensitive probe for the formation of stable coiled coil dimers than the absolute value of the molecular ellipticity at 222 nm alone.

Myc-LZ. Figure 2A (see also Table 1) shows CD spectra of Myc-LZ at different pH values and, for comparison, a spectrum recorded in a 1:1 water/TFE mixture. Approximately an equal amount of helicity is found in water independently of the pH, with a small increase at low pH values. More than a 50% increase is observed instead in TFE, a solvent that induces helicity in monomeric polypeptides with helical periodicity but disrupts tertiary and quaternary structures of α-helical aggregates (Lau et al., 1984). The effect of salt was screened, adding various salts chosen from different positions of the Hofmeister scale. At acidic pH, the addition of any salt results in a clear increase of both helicity and degree of coiling. Maximal effect is noticed with the addition of sulfate, independently of the nature of the cation. Comparison of the spectra in TFE and water at pH 3.0 in the presence of salt (Figure 2A,B) shows a clear relative change of the band intensities at 208 and 222 nm. Starting from 0.96 in TFE, it increases progressively up to a value greater than 1 (1.04) in the presence of $MgSO_4$. This behavior is entirely consistent with similar examples described in the literature

Table 1: Percentage of α-Helical Secondary Structure Determined by CD Measurements at 17 °C under Various pH and Salt Conditions[a]

pH	medium	helical content %
	Section A: Myc-LZ	
3.1	no salt	41
3.1	100 mM NaF	57
3.3	50 mM Na_2SO_4	76
3.0	50 mM $MgSO_4$	73
7.4	no salt	39
7.4	100 mM NaCl	41
7.4	100 mM $MgSO_4$	35
3.4	50% TFE, 50 mM Na_2SO_4	91
	Section B: TFEB-LZ	
3.8	no salt	30
3.6	100 mM NaF	30
3.2	50 mM $NaSO_4$	30
6.8	no salt	41
6.7	100 mM NaF	41
6.8	50 mM Na_2SO_4	41
6.9	50 mM $MgSO_4$	41
7.0	50% TFE	85

[a] For the measurements in aqueous solution, the peptide concentrations were 1 mM for Myc-LZ and 200 μM for TFEB-LZ, respectively. The data in TFE were collected at a concentration of 1 mM for both peptides.

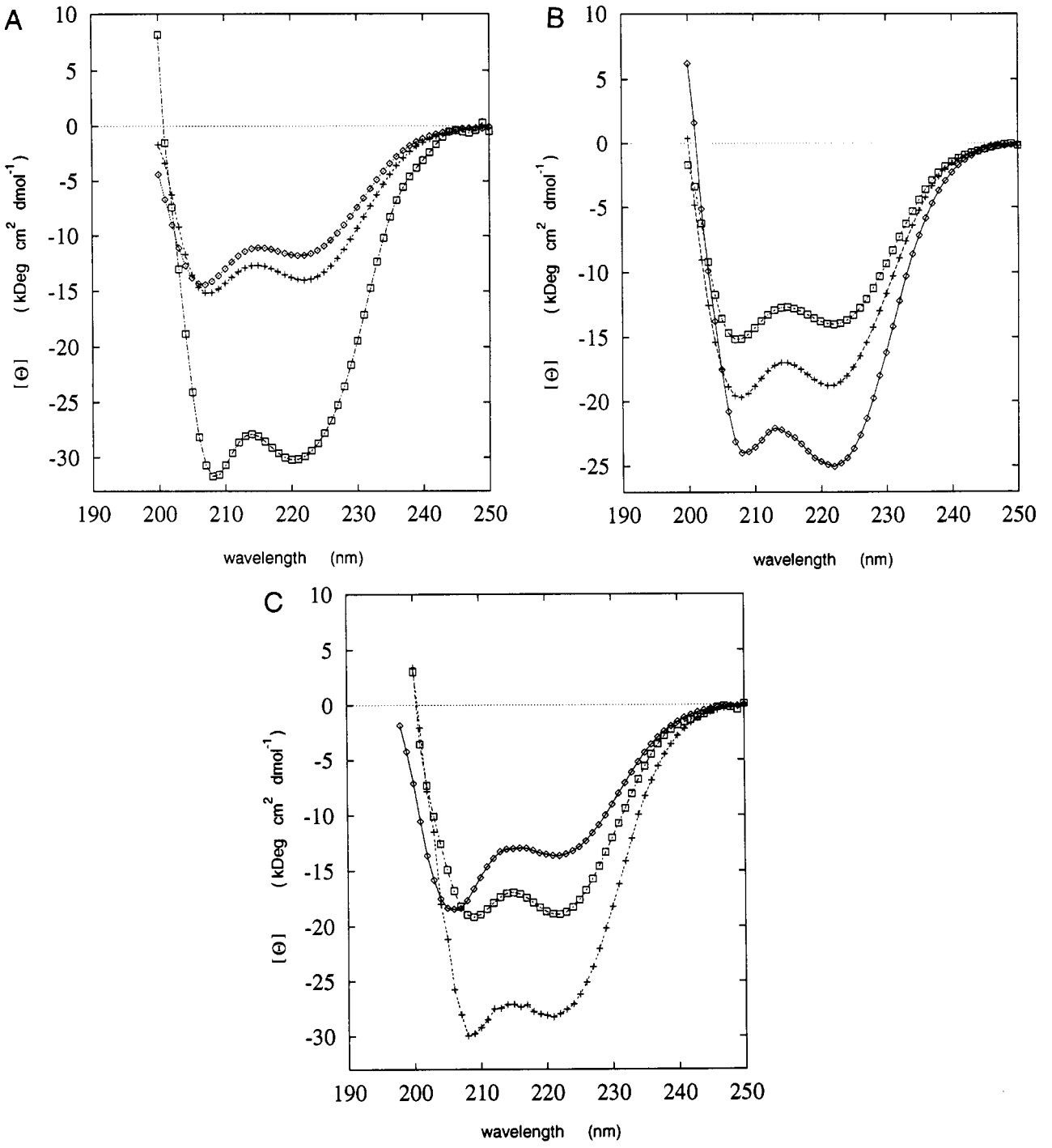

FIGURE 2: Effect of pH and salt on the circular dichroism spectra of the two peptides at 17 °C, 1 mM concentration. (A) pH effect on Myc-LZ; spectra recorded in water at pH 7.4 (◊) and pH 3.1 (+) and water/TFE (1:1) and 50 mM Na_2SO_4 (□). (B) Salt effect on Myc-LZ: Spectra recorded at pH 3.1 in the absence of salt (□) and in the presence of 100 mM NaF (+) and 50 mM Na_2SO_4 (◊). (C) pH effect on TFEB: Spectra recorded in water at pH 3.8 (◊) and pH 6.8 (□) and water/TFE (1:1) (+).

(Monera et al., 1993; Greenfield & Hitchcock-DeGregori, 1993) and may correspond to the conversion of an isolated α-helix, as expected to be present in TFE, to an α-helical coiled coil structure in aqueous solution. No salt effect was observed at pH 7 (Table 1, Section A).

CD spectra recorded at different peptide concentrations show that a clear concentration dependence effect is observable only in the presence of salt under acidic conditions (compare Figure 3, panels A and B).

Concentration dependence of the Myc-LZ peptide was further studied by recording thermal denaturation curves at different concentrations. The thermal denaturation curve recorded at 222 nm both at acidic (without salt) and neutral conditions showed no discernible cooperative transition over the range of 20 μM to 1 mM, and no dependence of the melting temperature on concentration could be detected. As an example, a plot of the variation of ellipticity at 222 nm vs the temperature recorded at neutral pH is shown in Figure 3C. On the other hand, measurements at acidic pH but in the presence of $MgSO_4$ indicate a cooperative concentration-dependent transition (Figure 3D). The midpoint of the transition T_m as determined by the maximum of the first derivative of the melting curve is 21, 35, and 44 °C for 20 μM, 200 μM, and 1 mM, respectively.

These data show that Myc-LZ has indeed the ability to adopt a well-defined and relatively stable α-helical secondary

Table 2: Proton Chemical Shifts

residue	chemical shifts (ppm) HN	Hα	Hβ	Hγ	Hδ	Hε/others
		Section A: Myc-LZ, 17 °C, pH 3.0				
Ser 1		4.11	3.92			
Val 2	8.66	3.96	1.94	0.82		
Gln 3	8.51	4.09	2.27	1.96, 1.91		6.80, 7.52
Ala 4	8.23	4.11	1.30			
Glu 5	8.17	4.11	2.37	1.98		
Glu 6	8.19	4.08	2.378	1.98		
Gln 7	8.13	3.98	2.29	1.97		
Lys 8	7.95	4.02	1.74	1.37	1.25	2.83
Leu 9	7.78	4.08	1.63	1.52	0.79, 0.73	
Ile 10	7.94	3.76	1.76	1.48, 1.08	0.80, 0.69	
Ser 11	8.20	4.21	3.94, 3.86			
Glu 12	8.22	4.05	2.43	2.12, 2.02		
Glu 13	8.30	3.96	2.46, 2.38	2.10, 1.95		
Asp 14	8.25	4.34	2.84, 2.68			
Leu 15	7.85	3.97	1.51	1.60	0.77	
Leu 16	7.87	4.08	1.68	1.56		
Arg 17	7.90	3.86	1.84	1.65, 1.47	3.11	7.17
Lys 18	7.88	3.95	1.79	1.29	1.45	2.83
Arg 19	8.04	4.03	1.81, 1.67	1.55	3.05	7.13
Arg 20	8.05	3.98	1.82, 1.68	1.47	3.05	7.16
Glu 21	8.03	3.99	2.01, 1.90	2.20		
Gln 22	8.05	4.01	2.03	2.41, 2.28		
Leu 23	7.91	3.94	1.47		0.79, 0.72	
Lys 24	7.85	3.97	1.69	1.54	1.35	2.84, 7.41
His 25	8.08	4.44	3.19, 3.12			7.19, 8.51
Lys 26	8.09	4.03	1.76	1.27	1.38	2.87
Leu 27	8.15	4.07	1.60	1.45	0.78, 0.71	
Glu 28	8.06	4.08	1.94	2.38, 2.30		
Gln 29	8.02	4.09	2.01	2.31, 2.39		
Leu 30	8.00	4.16	1.58	1.45	0.79, 0.73	
Arg 31	8.11	4.15	1.68	1.55, 1.46	3.06	7.07
Asn 32	8.28	4.60	2.74, 2.65			
Ser 33	8.12	4.27	3.80, 3.74			
		Section B: TFEB-LZ, 17 °C, pH 5.8				
Lys 1		4.00	1.89	1.45	1.67	2.96
Ser 2			3.85			
Arg 3	8.57	4.24	1.82, 1.72	1.58	3.12	
Glu 4	8.45	4.16	1.96, 1.88	2.22		
Leu 5	8.21	4.23	1.61	1.53	0.77, 0.87	
Glu 6	8.23	4.15	1.90	2.18		
Asn 7	8.32	4.56	2.73			7.56
His 8	8.41	4.64	3.23, 3.12			
Ser 9	8.26	4.26	3.85			
Arg 10	8.19	4.20	1.83, 1.72	1.58	3.12	
Arg 11	8.10	4.15	1.99	1.75, 1.53	3.07	
Leu 12	8.12	4.15	1.77, 1.64	1.46	0.80	
Glu 13	8.27	4.10	2.21	2.00, 1.93		
Met 14	8.09	4.42	2.02	2.47, 2.60		
Thr 15	8.28	4.34	4.20	1.21		
Asn 16	8.61	4.33	2.93, 2.73			7.66
Lys 17	8.07	4.11	1.84	1.63	1.51, 1.41	2.92
Gln 18	7.83	4.00	2.41	2.21, 2.04		7.43
Leu 19	8.22	3.97	1.61	1.18	0.66, 0.45	
Trp 20	8.18	4.34	3.32, 3.23			7.48, 10.08
Leu 21	8.00	3.97	1.78	1.51	0.87	
Arg 22	7.73	4.14	1.87, 1.78	1.68, 1.58	3.36, 3.03	
Ile 23	8.08	3.47		1.84	0.71, 0.83	
Gln 24	7.96	3.88	2.00	2.13		7.43
Glu 25	7.94	4.03	2.31	2.13		
Leu 26	8.18	3.98	1.68, 1.58	1.36	0.82, 0.67	
Glu 27	8.70	3.94	2.05, 1.90	2.48		
Met 28	7.92	4.16	2.15	2.64, 2.54		
Gln 29	7.98	4.04	2.51, 2.39	2.07		7.39
Ala 30	7.80	4.16	1.40			
Arg 31	7.64	4.15	1.86, 1.72	1.59	3.16	
Val 32	7.73	3.95	2.01	0.87, 0.75		
His 33	8.20	4.63	3.24, 3.13			
Gly 34	8.14	3.88				

structure with a helical content at least comparable to that of other monomeric helical peptides [for a review, see Scholtz and Baldwin (1992)]. However, all results presented in this section suggest that stabilization by dimer (or a higher aggregate) formation of Myc-LZ is induced only by salt under acidic conditions, that is, under nonphysiological conditions.

TFEB-LZ. Figure 2C shows CD spectra of TFEB-LZ at 1 mM concentration under various conditions. Whereas increasing the ionic strength of the solution has no significant effect on the stability (see Table 1, Section B), raising the pH from acidic to neutral value leads to an approximately 1.4-fold increase in α-helicity. In addition, the ratio of the two minima at 222 and around 208 nm changes (Figure 2C) from 0.73 (pH 3.6) to 1.00 (pH 6.9), but the effect is less evident than for Myc-LZ. Helicity shows a 30% increase to a total amount of about 85% upon addition of 50% TFE. The CD spectrum of the peptide in TFE shows again a more intense band at 208 nm than at 220 nm, indicative of a switch from interacting helices to a monomeric helix.

To determine if the increase of the helicity at neutral pH is associated with dimer formation, concentration-dependent thermal unfolding of TFEB-LZ was performed at pH 3.5 and 7.5 (Figure 4A,B). Although at acidic pH a slight dependence of the intensity at 222 nm can be detected, the effect at neutral pH is much more pronounced. Thermal denaturation studies at neutral pH (Figure 4C) showed, as expected, a concentration-dependent T_m ranging from 28 °C at 200 μM to 37 °C at 1 mM. The sharp kink of the curve at 1 mM concentration observed around 50 °C is caused by some peptide aggregation with consequent precipitation. At 20 μM the transition was broader, indicating a high percentage of monomeric peptide (data not shown). This prevents the possibility to delimit the beginning and the end of the transition and, therefore, estimation of a reliable value of T_m.

Unlike Myc-LZ, TFEB-LZ is able to adopt an ordered, concentration-dependent α-helical secondary structure at neutral pH and independently of salt concentration.

Ultracentrifugation. Ultracentrifugation experiments were only performed with TFEB-LZ since Myc-LZ does not contain aromatic residues and cannot be monitored easily by absorption spectroscopy. Figure 5 shows typical experimental absorbance profiles $A(r)$ for TFEB-LZ at sedimentation equilibrium, both in 50 mM Tris-HCl, pH 7.2, and in 50 mM sodium acetate at pH 3.8. The figure shows the results of least squares fits to the experimental data based on the assumption that the monomer and the dimer of TFEB-LZ are the only particles present. In addition, the figure shows the calculated radial distribution of the two components. It is apparent that the model fits the data with high accuracy and that both species contribute significantly to $A(r)$. Significant contribution of higher oligomers to the $A(r)$ profiles could be ruled out. Thus, a tetrameric species can contribute, at maximum, only 2% of the total amount of protein in the sample of Figure 5A and 0.2% in that of Figure 5B. In order to establish whether the dimers of TFEB-LZ are stable or linked to the monomers in an association equilibrium, several experiments at different loading concentrations or sample volumes were performed. It was found that, at a fixed pH value, the monomer/dimer distributions could be characterized by a common association constant, K_{12}, independently of the experimental conditions. On the other hand, K_{12} strongly increased with increasing pH. The values for K_{12} calculated at pH 3.8 and 7.2 are 1.6×10^3 and 15.4×10^3 M^{-1}, respectively, with an error of approximately 10% each. It follows that TFEB-LZ is present in solution as an equilibrium between monomers and dimers.

Secondary Structure Assignment by NMR. Detailed characterization of the secondary structure was undertaken by NMR. Complete sequence specific assignment of the resonances was obtained by standard methods using TOCSY

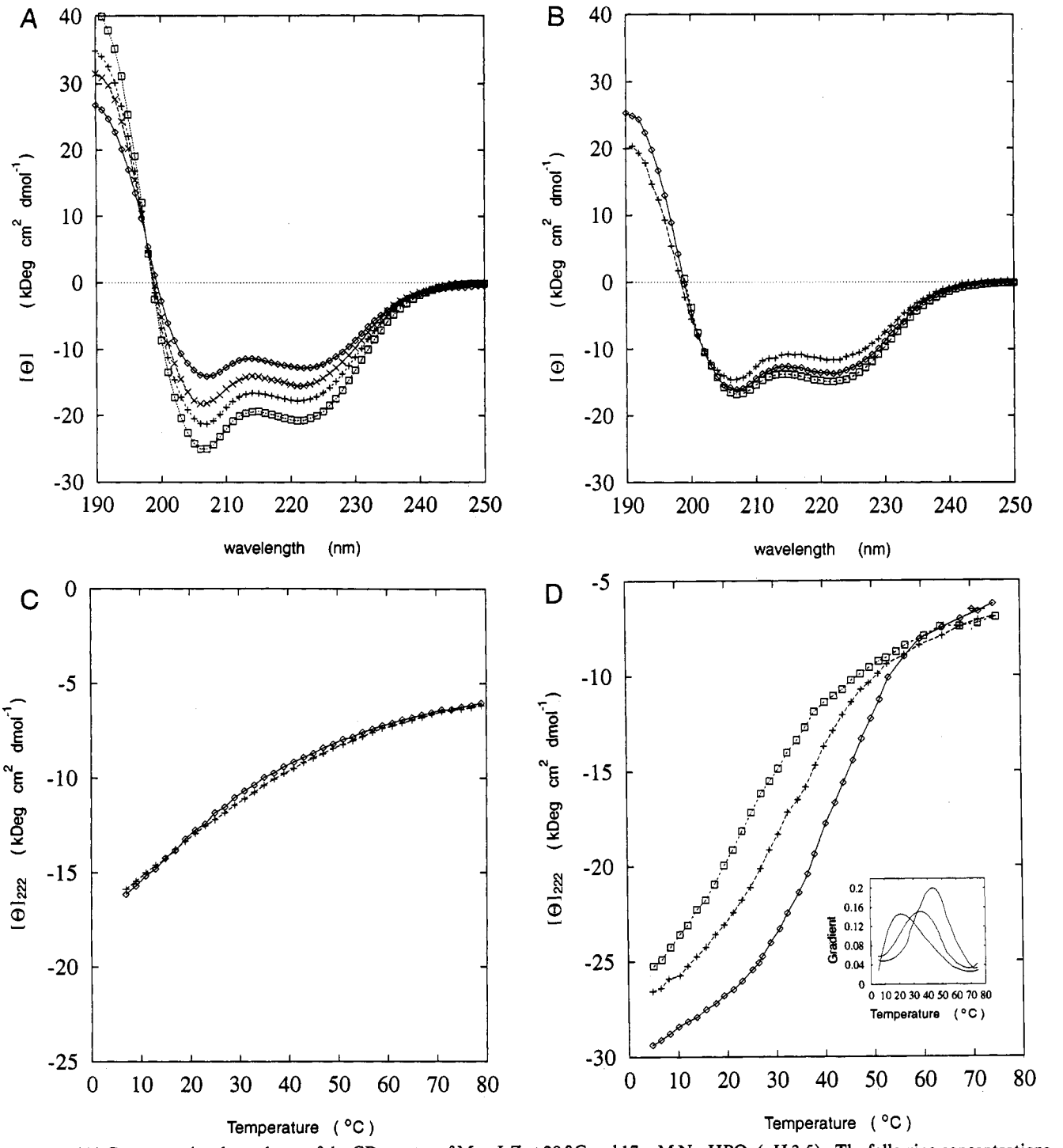

FIGURE 3: (A) Concentration dependence of the CD spectra of Myc-LZ at 20 °C and 17 mM Na_2HPO_4 (pH 3.5). The following concentrations correspond to the different symbols: 1.5 (◊), 35 (×), 150 (+), and 375 μM (□). (B) Concentration dependence of the CD spectra of Myc-LZ at 20 °C and 20 mM Tris-HCl (pH 7.5). The following concentrations correspond to these symbols: 3 μM (+), 30 μM (◊), and 2.5 mM (□). (C) Temperature dependence of the mean residue ellipticity (Θ) at 222 nm of Myc-LZ at pH 7.0 and 20 mM NaF. Peptide concentrations are 650 (◊) and 270 μM (+). (D) Temperature dependence of the mean residue ellipticity (Θ) at 222 nm of Myc-LZ at pH 3.1 and 50 mM $MgSO_4$. Peptide concentrations were 20 μM (□), 200 μM (+), and 1 mM (◊). Inset: First derivative of the temperature dependence curves. The maximum of the first derivatives shows a clear concentration dependence.

and NOESY 2D NMR experiments (Wüthrich, 1986). Spectra were recorded under different pH (3.0 and 5.8) and temperature conditions. No major changes of the overall conformation were detectable. Optimal conditions for the observation of amide proton connectivities (Wüthrich, 1986) were found at 17 °C and pH 5.8 for TFEB-LZ and pH 3.0 for Myc-LZ. Spectra of Myc-LZ at pH 5.8 showed very few NOE connectivities involving the amide protons as a consequence of their unfavorable exchange rate. This is consistent with the relatively low percentage of helicity of this peptide at both acidic and neutral pH.

The starting point for the assignment was the identification of unique spin systems in the TOCSY experiments (His, Ala, Asp). For TFEB-LZ, two of the Gln residues could be identified by NOESY H_2N/HN cross peaks. Spin systems were placed in the sequence by combining both the HN/HN and the Hα/HN connectivities. Additional cross peaks connecting Hβ/HN, Hα/Hβ, and Hγ/HN confirmed the

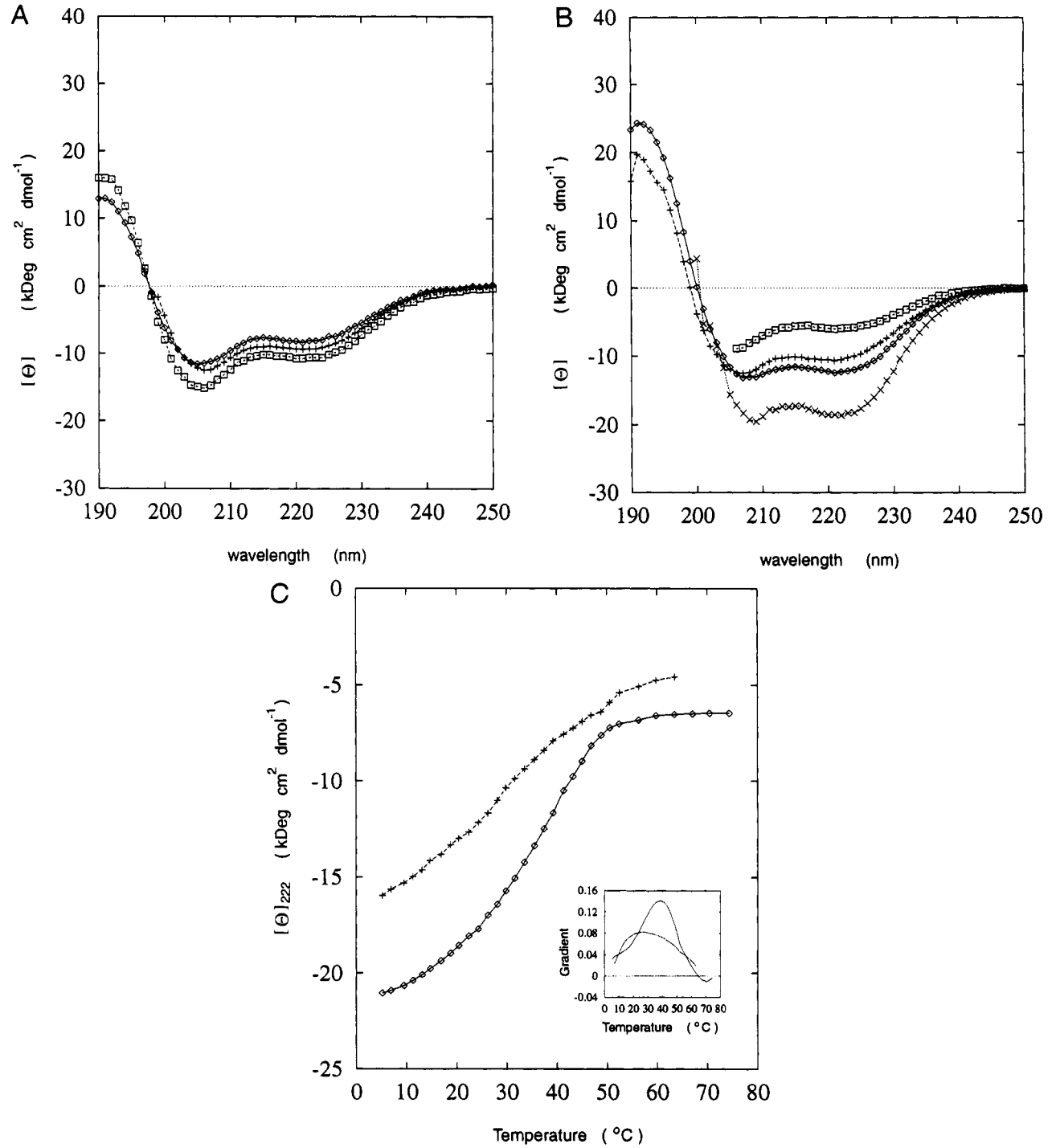

FIGURE 4: (A) Concentration dependence of the CD spectra of TFEB-LZ at 20 °C and 17 mM Na_2HPO_4 (pH 3.5). The following concentrations correspond to the different symbols: 1.2 μM (◇), 2.4 μM (+), and 1.2 mM (□). (B) Concentration dependence of the CD spectra of TFEB-LZ at 20 °C and 20 mM Tris-HCl (pH 7.5). The following concentrations correspond to the different symbols: 1.2 μM (□), 24 μM (+), 240 μM (◇), and 1 mM (×). (C) Temperature dependence of the mean residue ellipticity (Θ) at 222 nm of TFEB-LZ in water at pH 7.0. Peptide concentrations were 200 μM (+) and 1 mM (◇). Inset: First derivative of the temperature dependence curves.

assignment. The amide proton resonance regions of NOESY spectra of both the TFEB-LZ and the Myc-LZ peptides are shown in Figure 6.

Several sources of evidence (the relative intensities of the intraresidue and sequential Hα/HN cross peaks and HN/HN(i,i+1), the presence of several Hα/HN(i,i+3), Hα/HN(i,i+4), and Hα/Hβ(i,i+3) connectivities, and the upfield shifts of the Hα resonances from the corresponding values in a random coil) combine to indicate the presence of a well-defined helical structure in both peptides. A summary of the short- and medium-range NOEs as well as of the amide exchange rates is shown in Figure 7. The secondary structure of the two peptides is not identical. Myc-LZ shows an uninterrupted helix spanning the entire sequence. In contrast, residues 1–8 of TFEB-LZ are mostly in an extended conformation (the NH/NH(i,i+1) connectivities are very weak compared with the rest although still detectable at long mixing times) and helical thereafter. This provides an additional explanation for the CD results in TFE where TFEB-LZ exhibits a 30% increase in helicity (see above). This increase could mean that the percentage of molecules in helical conformation has increased leaving the percentage of helicity of each molecule unchanged. It could also mean, however, that the helical region of each molecule has been stabilized

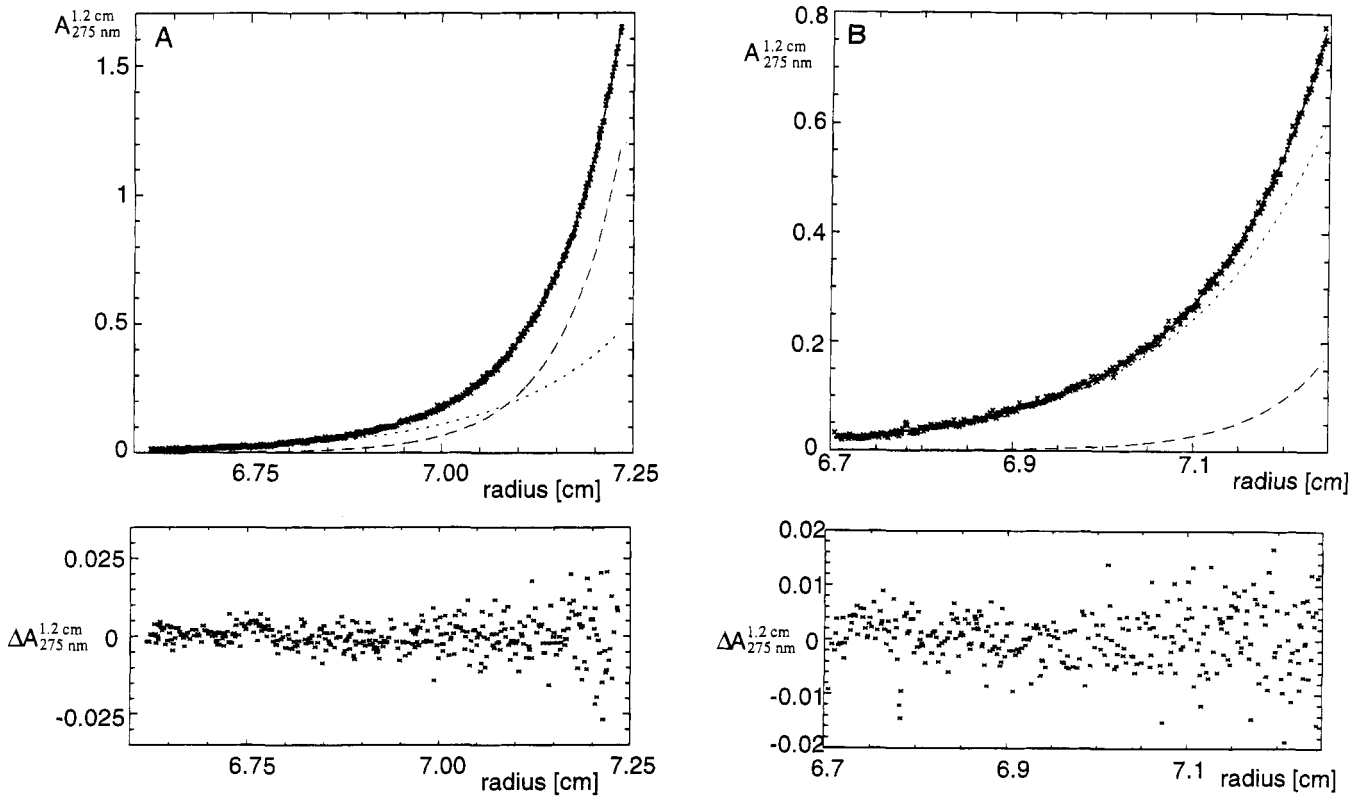

FIGURE 5: Analytical ultracentrifugation of TFEB-LZ. The concentration distribution is shown by crosses as a function of the radial position of TFEB-LZ. Upper plots: (×) Experimental absorbance-profiles $A(r)$ of TFEB-LZ in (A) 50 mM Tris-HCl, pH 7.2, 10 mM NaCl, loading concentration 84 μM ($A^{1.2cm}_{275nm}$ = 0.45) and (B) 50 mm of sodium acetate, pH 3.8, 20 mM NaCl, loading concentration 47 μM ($A^{1.2cm}_{275nm}$ = 0.25) in sedimentation equilibrium at 40000 rpm, 4 °C. The plot also shows the calculated distribution of monomer (···) and of dimer (– –) under both conditions. Lower plots: Local differences $\Delta A(r)$ between experimental and calculated values.

and extended such that the first seven residues (about 30% of the total residue number) are also in α-helical conformation.

Amide proton exchange confirms the different behavior of the N-termini of the two peptides. 2D spectra recorded immediately after dissolving TFEB-LZ in D_2O show that the resonances of the amide protons from the first 15 residues disappear too quickly to be recorded. Of the remaining amide protons, those of residues 16–24 can still be detected after 8 h in D_2O at 17 °C. For Myc-LZ peptide, the amide protons of residue 9–11, 15–19, and 22–23 are detectable for 2 h after dissolving the sample in D_2O at 17 °C. Only the amides of residues 10, 15, 17, and 18 can still be detected after 4 h in D_2O, and they vanish thereafter.

A detailed analysis of the spectra does not show any long-range connectivities as expected for a symmetric parallel coiled coil. As is now well understood, this type of structure produces no backbone contacts further apart than i–i+4 (i–i+5 for a few side chain–side chain contacts) since residues in the interface are packed onto their 2-fold related images (Saudek et al., 1990, 1991; Ellenberger et al., 1992). As a consequence of the symmetrical arrangement of two helices, it is impossible to distinguish a priori intermolecular from intramolecular effects. This has for some time hindered the determination of the three-dimensional structure of leucine zippers in solution from NOE data directly. It has however been demonstrated that, if the stoichiometry of the helix bundle can be determined independently, modeling may nevertheless lead to a quite accurate description of its structure (Saudek et al., 1990; Nilges & Brünger, 1993). Recently, an iterative computational strategy to overcome the problem has also been suggested (Nilges, 1993). Since our present interest is focused on the factors determining the stability of a coiled coil rather than on the structure, attempts to determine the 3D structure of the two peptides would not provide any additional information.

DISCUSSION

The data presented in this work show that the HLH-LZ zippers on their own can adopt relatively stable secondary structure. Under all conditions, both peptides studied are helical. Differences in the secondary structure of the two peptides observed by NMR are consistent with the different lengths and structural propensities of the linkers to the HLH domain (Figure 1A). The first seven residues of TFEB-LZ represent an insertion between the second helix of the HLH domain and the start of the LZ domain. Correspondingly, they show little helicity in the studied fragment as demonstrated by NMR. The Myc leucine zipper should, on the other hand, be a direct extension of the HLH region as shown in the Max crystal structure (Ferré-D'Amaré et al., 1993). However, aggregation of these helices into a coiled coil is strongly dependent upon pH. The dimers are far less stable than is the case for other well-characterized coiled coils, specifically those of the b-ZIP family (O'Shea et al., 1989a,b; Saudek et al., 1990; Junius et al., 1993). It is interesting to consider potential factors which stabilize both the monomeric and the dimeric structure.

Factors Influencing the Stability. It is by now established that coiled coil stability increases with the number of heptads and of favorable hydrophobic and electrostatic interactions involving the *a* and *d* heptad positions, which are centered in the dimer interface, and the *e* and *g* positions, which flank the interface (Cohen & Parry, 1990; Ellenberger et al., 1992; Zhou et al., 1992a,b; Monera et al., 1993). The minimum length of a synthetic peptide required to form a stable, dimeric

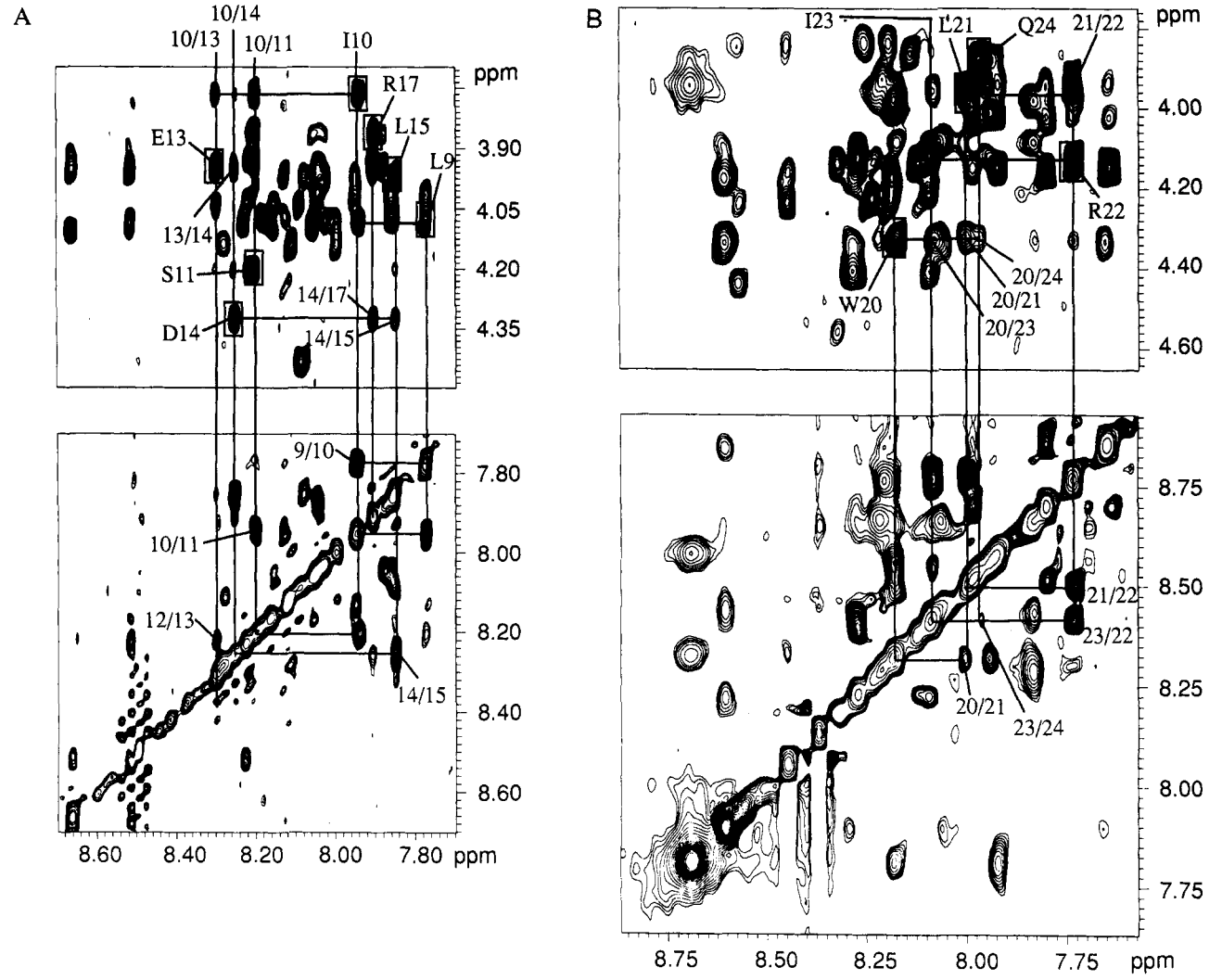

FIGURE 6: Parts of the NOESY spectra of the two peptides with a mixing time of 200 ms. (A) Myc-LZ in H_2O at pH 3.1 and 290 K, 2.0 mM peptide concentration. (B) TFEB-LZ in H_2O at pH 5.8 and 300 K, 2.5 mM peptide concentration. The upper sections show the fingerprint region and the lower sections show the NH–NH region. For reasons of clarity, only some of the intra- and interresidual NOE connectivities between Hα and NH resonances are labeled with the sequence number of the residues involved. Intraresidual NOEs are indicated by boxes and labeled with the single-letter code and sequence number of the amino acid.

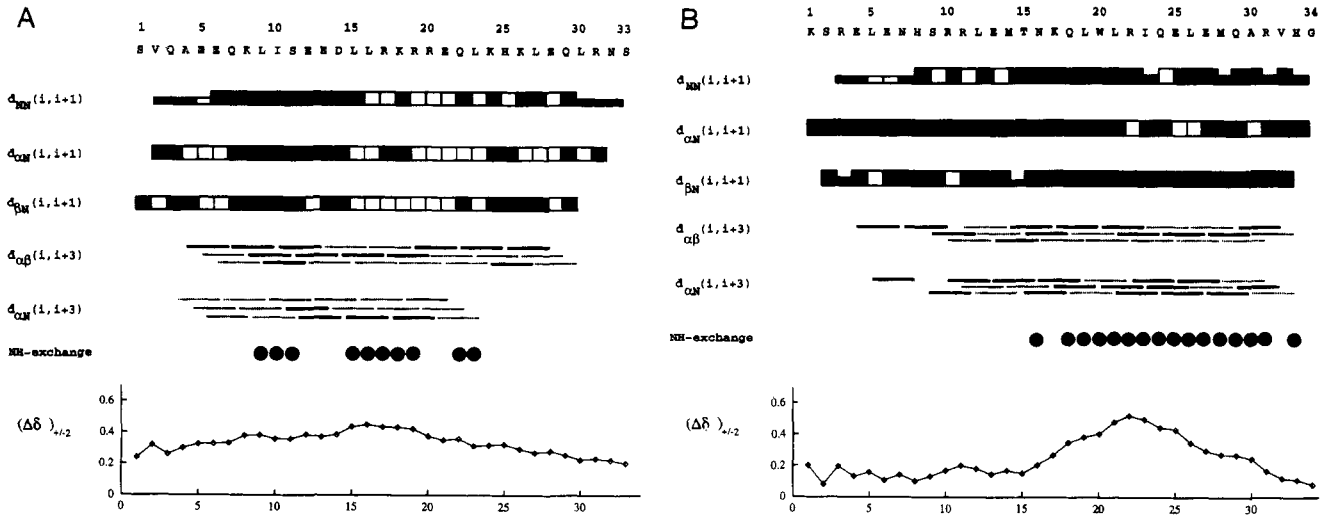

FIGURE 7: Survey of the sequential and other interresidual distances observed for (A) Myc-LZ and (B) TFEB-LZ. The intensity of the NOEs is indicated by the height of the bars. Unshaded bars or thin lines indicate ambiguous NOEs due to spectral overlap. Filled circles indicate the position of the slowly exchanging HN hydrogens (after 2 h in the case of Myc-LZ and 4 h in the case of TFEB-LZ) in D_2O. The deviation of the chemical shifts of the $C^{\alpha}H$ resonances from random coil values is shown underneath after smoothing using a window of ±2 residues (Pastore & Saudek, 1991; Wishart et al., 1991). Positive values are typical of helical structures.

α-helical coiled coil is considered to be around 29 residues, *i.e.*, four heptad repeats (Lau et al., 1984). While Myc-LZ comprises four entire repeats, TFEB-LZ is observed by NMR to be helical only from residue 8 to the end (26 residues) and,

thus, is one helical turn shorter than the minimum length. The minimum number of hydrophobic contacts required to stabilize the dimer might therefore not be present. On this basis alone, a low stability of this peptide dimer would be expected.

The arrangement of the TFEB-LZ and Myc-LZ sequences in an α-helical structure is shown schematically in a helical wheel representation (Figure 1B,C). The hydrophilic nature of the residues at the *a* heptad position may not favor dimerization in either peptide. In TFEB-LZ, the *a* positions are occupied by Ser, Asn, and Ala, none of which guarantees close hydrophobic packing in a dimer. Substitution of leucines with alanines in *a* position leads to significant reduction of the coiled coil stability (Zhou et al., 1992a,b). In Myc-LZ, two of the *a* positions are occupied by Glu and one by Arg. The *d* positions retain their character of strong hydrophobicity, common also to the b-ZIP family, except for a His located in the *d* position seven residues C-terminal to the last Leu in TFEB. Yet, a similar case occurs in Jun and Fos where His-200 is similarly located one heptad C-terminal from the fifth leucine. Schuermann et al. (1991) showed that mutations at this position strongly destabilize dimerization. The *e* and *g* positions are often occupied by charged residues which are thought to interact electrostatically and to form salt bridges between the helices, as shown by mutagenesis studies of the GCN4 coiled coil region (O'Shea et al., 1992) and the X-ray structure of the GCN4-LZ (O'Shea et al., 1991). In TFEB-LZ, only two intramolecular *e*–*g* salt bridges are possible in comparison with the three present in the GCN4-LZ. The sequence of Myc-LZ contains a complicated pattern of positively and negatively charged residues at the dimer interface. While the N-terminus contains four Glu in *g* and *a* positions, in the C-terminus *e* and *g* positions are occupied by Arg and Lys. Because of electrostatic repulsion in the interface at any pH value, homodimer formation is strongly destabilized. Addition of salts at a pH value where the acidic residues are not protonated may counterbalance the positive charges and facilitate dimerization (Monera et al., 1993; Zhou et al., 1994).

Role of LZ in HLH Proteins. As described for the b-ZIP family, conclusions derived from studies on isolated leucine zipper peptides appear to be applicable to the intact proteins. Indeed, the data presented in this paper are fully consistent with the different homodimerization properties of the Myc and TFEB proteins. As TFEB-LZ homodimerizes at neutral pH as demonstrated by our data, likewise the full-length TFEB protein is able to homodimerize at physiological pH. Myc, on the other hand, is unable to form homodimers under neutral conditions. Myc-LZ clearly reflects this behavior, since homodimerization is detected only at acidic pH.

From our results and mutagenesis studies described in the literature, the HLH-LZ family may be subclassified according to the main role played by the leucine zipper domain. The behavior of Myc and TFEB may be chosen as a paradigm for each subfamily. In the TFEB subfamily, the leucine zipper region contributes to the dimerization energy of the entire motif without being essential to the choice of the partner. Deletion studies of the leucine zipper region of the TFEB have shown that it is essential for dimerization (Fisher et al., 1991). Although it has been shown that TFEB heterodimerizes with TFE3, the leucine zippers of TFEB and TFE3 contain equally charged residues in the *e* and *g* positions so that *e*–*g* interactions could not account for discrimination between hetero- and homodimerization. The TFEB–TFE3 heterodimer binds to DNA with an affinity comparable to either homodimer (Fisher et al., 1991).

On the other hand, the dimerization properties of the Myc-LZ are reminiscent of the leucine zippers of the Fos protein, which also homodimerizes poorly and preferentially forms heterodimers with Jun, another member of the same family. Fos-LZ homodimerization could be nevertheless demonstrated at acidic pH even in the absence of salt (O'Shea et al., 1992). Like Foc, Myc is found preferentially *in vivo* as a heterodimer. In the dimerization partner, Max, four out of six corresponding *e* and *g* positions in the leucine zippers are occupied by oppositely charged residues which would increase the stability of the heterodimer. In the two other positions, positively charged *e* residues in Myc are juxtaposed to Gln at *g* positions in Max. Mutagenesis studies systematically exchanging *e* and *g* positions in the leucine zippers of Myc and Max (Amati et al., 1993) proved that these positions govern dimerization specificity. The resulting proteins had inverted dimerization specificities. Therefore, in the Myc subfamily in which heterodimerization is strongly favored over homodimerization, the main role of the leucine zippers is to specify the dimerization partner.

To gain further insight into heterodimer formation, we are currently investigating the homodimerization of Max-LZ and its heterodimerization with Myc-LZ.

ACKNOWLEDGMENT

We are grateful to Dr. R. De Francesco for performing preliminary CD measurements and Dr. J. H. Lakey for technical support with CD and helpful discussions. We would also like to thank Drs. A. Atkinson, P. Brownlie, M. Pfuhl, and A. Politou for critical reading of the manuscript and extensive discussions.

REFERENCES

Alberti, S., Oehler, S., von Wilcken-Bergmann, B., & Müeller-Hill, B. (1993) *EMBO J. 12*, 3227–3236.
Amati, B., Brooks, M. W., Levy, N., Littlewood, T. D., Evan, G. I., & Land, H. (1993) *Cell 72*, 233–245.
Bairoch, A., & Boeckmann, B. (1991) *Nucleic Acids Res. 19*, 2247–2249.
Bax, A., & Davis, D. G. (1985) *J. Magn. Reson. 65*, 355–360.
Baxevanis, A. D., & Vinson, C. R. (1993) *Curr. Opin. Genet. Dev. 3*, 278–285.
Beckmann, H., & Kadesch, T. (1991) *Genes Dev. 5*, 1057–1066.
Beckmann, H., Su, L.-K., & Kadesch, T. (1990) *Genes Dev. 4*, 167–179.
Carr, C. S., & Sharp, P. A. (1990) *Mol. Cell. Biol. 10*, 4384–4388.
Cao, Z., Umek, R. M., & McKnight, S. L. (1991) *Genes Dev. 5*, 1538–1552.
Chen, Y.-H., Yang, J. T., & Chau, K. H. (1974) *Biochemistry 13*, 3350–3359.
Cohen, C., & Parry, D. A. D. (1990) *Proteins 7*, 1–15.
Cooper, T. M., & Woody, R. W. (1990) *Biopolymers 30*, 657–676.
Dang, C. V., McGuire, M., Buckmire, M., & Lee, W. M. F. (1989) *Nature 337*, 664–666.
Davis, R. L., Cheng, P.-F., Lassar, A. B., & Weintraub, H. (1990) *Cell 60*, 733–746.
Ellenberger, T. E., Brandl, C. J., Struhl, K., & Harrison, S. C. (1992) *Cell 71*, 1223–1237.
Ferré-D'Amaré, A. R., Prendergast, G. C., Ziff, E. B., & Burley, S. K. (1993) *Nature 363*, 38–45.
Fisher, D. E., Carr, C. S., Parent, L. A., & Sharp, P. A. (1991) *Genes Dev. 5*, 2342–2352.
Frain, M., Swart, G., Monaci, P., Nicosia, A., Staempfli, S., Frank, R., & Cortese, R. (1989) *Cell 59*, 145–150.

Greenfield, N. J., & Hitchcock-DeGregori, S. E. (1993) *Protein Sci. 2*, 1263–1273.
Gregor, P. D., Sawadogo, M., & Roeder, R. G. (1990) *Genes Dev. 4*, 1730–1740.
Hai, T., Liu, F., Coukos, W. J., & Green, M. R. (1989) *Genes Dev. 3*, 2083–2090.
Hu, Y.-F., Lüscher, B., Admon, A., Mermod, N., & Tijan, R. (1990) *Genes Dev. 4*, 1741–1752.
Jeener, J., Meier, B. H., Bachmann, P., & Ernst, R. R. (1979) *J. Chem. Phys. 71*, 4546–4553.
Johnson, M. L., & Faunt, L. M. (1992) *Methods Enzymol. 210*, 1–37.
Junius, F. K., Weiss, A. S., & King, F. G. (1993) *Eur. J. Biochem. 214*, 415–424.
Landshulz, W. H., Johnson, P. F., & McKnight, S. L. (1988) *Science 240*, 1759–1764.
Lau, S. Y. M., Taneja, A. K., & Hodges, R. S. (1984) *J. Biol. Chem. 259*, 13253–13261.
Macura, S., Huang, Y., Suter, D., & Ernst, R. R. (1981) *J. Magn. Reson. 43*, 259–281.
Marion, D., & Wüthrich, K. (1983) *Biochem. Biophys. Res. Commun. 113*, 967–974.
Mitchell, P., & Tijan, R. (1989) *Science 245*, 371–378.
Monera, O. D., Zhou, N. E., Kay, C. M., & Hodges, R. S. (1993) *Biochemistry 268*, 19218.
Murre, C., Shonleber McCaw, P., & Baltimore, D. (1989) *Cell 56*, 777–783.
Nicosia, A., Monaci, P., Tomei, L., De Francesco, R., Nuzzo, M., Stunnenberg, H., & Cortese, R. (1990) *Cell 61*, 1225–1232.
Nilges, M. (1993) *Proteins 17*, 297–309.
Nilges, M., & Brünger, A. T. (1993) *Proteins 15*, 133–146.
Oas, T. G., McIntosh, L. P., O'Shea, E. K., Dahlquist, F. W., & Kim, P. S. (1990) *Biochemistry 29*, 2891–2894.
O'Shea, E. K., Rukowski, R., & Kim, P. S. (1989a) *Science 243*, 538–542.
O'Shea, E. K., Rukowski, R., Stafford, W. F., & Kim, P. S. (1989b) *Science 245*, 646–648.
O'Shea, E. K., Klemm, J. D., Kim, P. S., & Alber, T. (1991) *Science 254*, 539–544.
O'Shea, E. K., Rukowski, R., & Kim, P. S. (1992) *Cell 68*, 699–708.
Pastore, A., & Saudek, V. (1990) *J. Magn. Reson. 90*, 165–176.
Rance, M. (1987) *J. Magn. Reson. 74*, 557–564.
Reynolds, J. A., & McCaslin, D. R. (1985) *Methods Enzymol. 117*, 41–53.
Saudek, V., Pastore, A., Castiglione Morelli, M. A., Franck, R., Gausepohl, H., Gibson, T., Weih, F., & Roesch, P. (1990) *Protein Eng. 4*, 3–10.
Saudek, V., Pastore, A., Castiglione Morelli, M. A., Frank, R., Gausepohl, H., & Gibson, T. J. (1991) *Protein Eng. 4*, 519–529.
Scholtz, J. M., & Baldwin, R. L. (1992) *Annu. Rev. Biophys. Biomol. Struct. 21*, 95–118.
Schuck, P. (1994) *Prog. Colloid Polym. Sci. 94*, 1–13.
Schuermann, M., Hunter, J. B., Hennig, G., & Müller, R. (1991) *Nucleic Acids Res. 19*, 739–746.
Williams, S. C., Cantwell, C. A., & Johnson, P. (1991) *Genes Dev. 5*, 1553–1567.
Wishart, D. S., Sykes, B. D., & Richards, F. M. (1991) *J. Mol. Biol. 222*, 311–333.
Wüthrich, K. (1986) *NMR of Proteins and Nucleic Acids*, John Wiley & Sons, New York.
Zhou, N. E., Kay, C. M., & Hodges, R. S. (1992a) *J. Biol. Chem. 267*, 2664–2670.
Zhou, N. E., Zhu, B.-Y., Kay, C. M., & Hodges, R. S. (1992b) *Biopolymers 32*, 419–426.
Zhou, N. E., Kay, C. M., & Hodges, R. S. (1994) *J. Mol. Biol. 237*, 500–512.